Title
Energetics of Glutamate Binding to an Ionotropic Glutamate Receptor

Journal
The Journal of Physical Chemistry B, 121(46)

ISSN
1520-6106

Authors
Yu, Alvin
Lau, Albert Y

Publication Date
2017-11-22

DOI
10.1021/acs.jpcb.7b06862

Peer reviewed

HHS Public Access

Author manuscript

J Phys Chem B. Author manuscript; available in PMC 2017 December 05.

Published in final edited form as:

J Phys Chem B. 2017 November 22; 121(46): 10436–10442. doi:10.1021/acs.jpcb.7b06862.

Energetics of Glutamate Binding to an Ionotropic Glutamate Receptor

Alvin Yu[1,2] and **Albert Y. Lau**[1,2,*]

[1]Program in Molecular Biophysics, Johns Hopkins University, Baltimore, MD 21218, USA

[2]Department of Biophysics and Biophysical Chemistry, Johns Hopkins University School of Medicine, Baltimore, MD 21205, USA

Abstract

Ionotropic glutamate receptors (iGluRs) are ligand-gated ion channels that are responsible for the majority of excitatory transmission at the synaptic cleft. Mechanically speaking, agonist binding to the ligand binding domain (LBD) activates the receptor by triggering a conformational change that is transmitted to the transmembrane region, opening the ion channel pore. We use fully atomistic molecular dynamics simulations to investigate the binding process in the α-amino-3-hydroxy-5-methyl-4-isoxazolepropionic acid (AMPA) receptor, an iGluR subtype. The string method with swarms of trajectories was applied to calculate the possible pathways glutamate traverses during ligand binding. Residues peripheral to the binding cleft are found to metastably bind the ligand prior to ligand entry into the binding pocket. Umbrella sampling simulations were performed to compute the free energy barriers along the binding pathways. The calculated free energy profiles demonstrate that metastable interactions contribute substantially to the energetics of ligand binding and form local minima in the overall free energy landscape. Protein-ligand interactions at sites outside of the orthosteric agonist-binding site may serve to lower the transition barriers of the binding process.

Graphical abstract

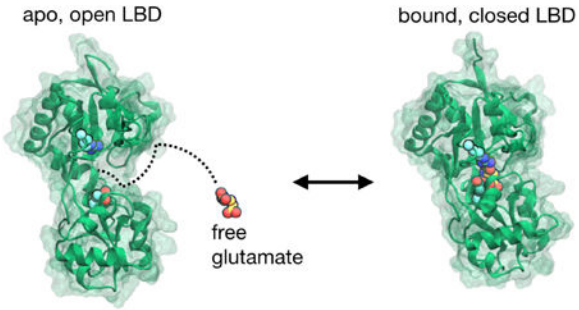

*Corresponding author: 443-287-4528, alau@jhmi.edu.

Author Contributions: A.Y. and A.Y.L. initiated the project, analyzed the data, and wrote the manuscript. A.Y. performed the calculations. All authors have given approval to the final version of the manuscript.

Notes: The authors declare no competing financial interest.

Introduction

In the brain, glutamate binding serves as an important signal for activation of downstream neurons.[1] α-Amino-3-hydroxy-5-methyl-4-isoxazolepropionic acid (AMPA) receptors, composed of an amino-terminal domain (ATD), a ligand-binding domain (LBD), a transmembrane domain (TMD), and C-terminal domain (CTD), sense the release of neurotransmitters at synaptic terminals.[2] Architecturally, AMPA receptors are tetrameric complexes arranged in a dimer-of-dimers fashion.[3] The binding of neurotransmitters triggers large structural rearrangements in which conformational change in the separate LBDs provides the necessary tension for opening the channel pore. Isolated LBDs close once glutamate binds. Thus, ligand binding and LBD closure are thought to be tightly coupled processes.

Many computational methods have been employed to study protein-ligand binding. Unbiased simulation[4,5] is the most straightforward approach and yields detailed information on the molecular mechanisms of the binding process, but it is also the most computationally expensive, often requiring the use of special purpose hardware[6]. Usually, because of the computational cost involved, only a limited number of binding events are sampled. Enhanced sampling methods, such as umbrella sampling and the string method, are an alternative approach.

For the AMPA receptor subtype, GluA2, umbrella sampling has been used to calculate the free energy of ligand binding for multiple agonists.[7] The energetics of cleft closure and ligand docking were evaluated separately. The contributions to the free energy from each was computed along a predetermined pathway, using biasing potentials to pull the system from a ligand-free, open LBD conformation to a ligand-bound, closed LBD conformation.

Here, we aim to re-examine glutamate receptor ligand binding using the string method[8,9]. In contrast to our previous study[7], translation of the ligand into the binding pocket is not restricted to a predetermined path, and ligand translation and protein conformational change are studied as coupled processes in concert. As a result, we find ligand-binding pathways that are physically more realistic and putative protein-ligand interactions that occur outside of the binding pocket.

Methods

Simulation System Preparation

The atomic model for the ligand bound monomer was constructed from the crystal structure of the GluA2 ligand-binding core (S1S2) in complex with glutamate (PDB ID: 1FTJ). The atomic model for the ligand-free monomer was constructed from the crystal structure of the GluA2 ligand-binding core (S1S2) in the apo state (PDB ID: 1FTO). Missing protein backbone was added to the model using the Modloop server[10], and missing sidechains were constructed using SCWRL4[11]. Models included the crystallographic waters from the binding cleft, and both systems were solvated with 13,836 water molecules. A glutamate molecule was added to bulk solvent in the apo system ~38 Å away from the LBD center of mass. Both systems were neutralized by adding Na^+ and Cl^- ions to the bulk solution until

the salt concentration reached 150 mM. Both systems contained a total of 45,723 atoms. Periodic boundary conditions were imposed on an orthorhombic cell with approximate dimensions of 84 Å × 68 Å × 78 Å. The systems were energy minimized and equilibrated at constant pressure and temperature (NPT) conditions at 1 atm and 300K with a time step of 2 fs. For all simulations, the all-atom potential energy function PARAM27[12,13] for proteins and the TIP3P potential energy function for water[14] were used. Electrostatic interactions were computed using the particle mesh Ewald (PME) algorithm, and short-range, non-bonded interactions were truncated at 12 Å. All productions runs were performed using CHARMM[15].

String Method Calculation

Conformational transitions in biological macromolecules are multi-dimensional processes that require the concerted movement along a large number of degrees of freedom. The important order parameters that well describe these transitions are often not known *a priori*. The string method is a "chain-of-states" approach that optimizes the transition states between two end points and has been used to characterize conformational change in tyrosine kinases, ion channels, and motor proteins.[16–19]

Briefly, the string method interpolates between two end states by sampling states intermediate to the transition.[8,9] The algorithm consists of first constructing an initial interpolation between the two end states to form a transition pathway. The pathway is then iteratively refined as follows until it converges: (1) each transition state is evolved using molecular dynamics simulations to estimate the instantaneous forces underlying the transition; (2) states are moved in the direction of those forces; (3) the entire pathway is reparametrized to maintain some metric to separate the states – typically this metric is taken to be the Euclidean distance in the space of collective variables. The two end states used in our study were taken from the prepared atomic models of the ligand-bound and ligand-free LBD monomers.

Three initial transition pathways were constructed based on the accessibility of the ligand to the binding pocket (Figure S1). In the interpolation for pathway 1, the ligand was translated into the binding cleft between K449 and S652 using biasing potentials. For the interpolations in pathways 2 and 3, glutamate was translated into the binding pocket via the ξ_1 and ξ_2 sides of the cleft respectively, where ξ_1 and ξ_2 are two center of mass distances between lobe 1 and lobe 2 (Figure 1), using biasing potentials. The total number of states, or images, for pathways 1, 2, and 3 were 129, 132, and 129, respectively. For the string method calculations, our collective variables were the Cartesian coordinates of all $C\alpha$ atoms of the LBD, and the two terminal carbonyl carbons and the $C\alpha$ atom of the ligand.

The string method algorithm with swarms of trajectories[9] was applied to all three pathways. Pathways 1 and 2 converged after ~225 ns of aggregate sampling. Pathway 3, however, did not converge after 258 ns of sampling and was discarded for being trapped along transition pathways in which optimization using the string method was slow. Timesteps of 2.0 fs and 1.0 fs were used in the free and restrained simulations, respectively. Each iteration of the string method involved the following: (1) 5,000 steps of restrained dynamics to push the pathway to the target collective variable values; (2) a short restrained dynamics run for 500

steps to generate the starting coordinates for the swarms– starting coordinates were written out at 5-step intervals; (3) 100 simulations of short 50-step unbiased simulations to measure the average drift of the swarms; (4) the average drift was measured, and the positions of the images were updated using the average drift; (5) the path was reparameterized, and the target collective variables were updated for the next iteration with the current position of each image. Convergence was assessed by summing the distances between the images at the *j*-th iteration and the images at the (*j+1)*-th iteration, i.e., $c_j=\sum_{i=1}^{N-1}\sqrt{(\vec{\theta}_{i,j}-\vec{\theta}_{i,j+1})^2}$ where $\vec{\theta}_{i,j}$ is a multi-dimensional vector representing the collective variables of image *i* at the *j*-th iteration.

The Free Energies of the Transition Paths

Once a pathway is found, part of the difficulty in capturing the free energy along a particular binding pathway stems from the high dimensionality of the ligand binding process. Protein-ligand interactions, ligand orientation, protein conformational change, and specific residue-residue contacts may each contribute to the free energy along different degrees of freedom.[20] To address this issue, we use umbrella sampling and choose a global order parameter, α, that measures the progress along the binding process. In the discrete case, as in our present study, α is an index over the states of the system defined by the transition states of a converged pathway identified by the string method. Ligand association can then be represented as a transition: $\alpha_N \rightarrow \alpha_{N-1} \rightarrow \ldots \rightarrow \alpha_1 \rightarrow \alpha_0$; where α_N corresponds to an initial state containing the protein and ligand separated by bulk solvent, and α_0 corresponds to a final state containing the ligand bound complex.

The parameter α may depend on many degrees of freedom that capture the conformation of the protein and ligand at the particular transition state of interest. Given the atomic coordinates of a protein-ligand system, how do we determine α and how far along the binding process a system is? In the present study, to address these questions, we compare the Cartesian coordinates of the Cα atoms in the protein to capture the protein conformation and residue-specific interactions, and two terminal carbonyl carbons as well as the Cα atom in the ligand to specify ligand orientation and protein-ligand interactions. The system is then assigned to the most similar state, α_i, along the 1-dimensional transition pathway. This is done automatically by first measuring the coordinates of interest at each α_i, Voronoi tessellating the phase space of those coordinates, and assigning each conformation in the neighborhood of α_i to the index *i* (see Figure S2 for exemplary figures related to an alanine dipeptide).

The free energy along the binding pathway can then be calculated by umbrella sampling. Voronoi tessellation has been previously used to separate the transition states.[21–23] Here, the same approach is taken, and statistics on the occupancies of each state are collected on a confined region of the 1-dimensional pathway through the use of biasing potentials. The biasing potentials restrain the system along the multi-dimensional coordinates of interest. Contributions of the biasing potential to the free energy can be unbiased using the Weighted Histogram Analysis Method (WHAM).[24,25] Thus, the method calculates a free energy

profile across a multidimensional surface. The accuracy of this PMF depends on the degree of sampling between each state, α_i, and its neighbors.

Umbrella sampling simulations, totaling 105 ns along pathway 1 and 103 ns along pathway 2, were performed to calculate the free energy profiles. Each image was harmonically restrained with force constants (0.01 kcal/mol/Å^2) at each of the collective variables from the string method. Biased distributions were collected across all collective variables. The phase space of the collective variables was Voronoi tessellated, using each image as the center for the Voronoi cell. The biased distribution of states along the binding pathway was calculated by assigning systems in the neighborhood of state *i* to state *i* based on the Voronoi tessellation, i.e.,

$$x \in \alpha_i \leftrightarrow \| \overrightarrow{\theta}(x) - \overrightarrow{\theta}(\alpha_j) \| \geq \| \overrightarrow{\theta}(x) - \overrightarrow{\theta}(\alpha_i) \|, \forall j \neq i,$$

where *x* represents a conformation of the system collected during the umbrella sampling, α_i is the system at image index *i*, and $\vec{\theta}(x)$ is a multidimensional vector containing the collective variable values of conformation *x*. The biased distributions were unbiased using WHAM.

Results and Discussion

Local optimization of metastable binding intermediates

Binding along converged pathways 1 (Figure 2) and 2 (Figure 3) contains distinct interactions with residues on the periphery of the LBD cleft that are not directly in the binding pocket. The presence of multiple binding pathways suggests that ligand binding is not restricted to a single pathway. In pathway 1, the ligand forms interactions with R684 (Figure 2C) and K449 (Figure 2E), whereas in pathway 2, the ligand forms interactions with R453 (Figure 3C) and R661 (Figure 3E). In particular, R453 and R684 pass the ligand to R660 and K449, respectively, prior to binding (Figure 2 C–E, Figure 3 C–E). R660 and K449 form metastable interactions with the ligand before passing it into the pocket. Once inside the pocket, the ligand contacts Y450 and R485 on lobe 1, and E705 on lobe 2, as the LBD closes.

Specific residues were observed to be involved in locking the LBD closed. Consistent with previous crystal structures, the D651-S652 peptide bond flips to form additional hydrogen bonding interactions between lobe 1 and lobe 2 of the LBD; the backbone carbonyl group of S652 (lobe 2) hydrogen bonds with the backbone amine of G451 (lobe 1).[26] A salt bridge between K730 and D728 in the hinge region of the LBD also forms after the ligand settles into the binding pocket. The interaction between K730 and D728 may be correlated with the degree of cleft closure. This salt bridge forms once the LBD is closed to (ξ_1, ξ_2) = (11.9, 11.4 Å) in pathway 1 and to (ξ_1, ξ_2) = (9.5, 5.3 Å) in pathway 2. A comparison of crystal structures of apo and glutamate-bound LBDs shows K730 forms a salt bridge with E705 in the apo state; however, once a ligand binds, K730 switches interaction partners to D728.[26]

This interaction may be minor compared with cross-lobe interactions, however, since several antagonist bound crystal structures do not show this switching mechanism.[26–28]

Characterizing the energetics of molecular interactions along a binding pathway

We computed the free energy profile along each of the converged binding pathways obtained with the string method. In pathway 1 (Figure 4), the free energy plateaus when the protein and ligand are separated by ~12 Å of solvent (i = 90) and oscillates around 7-8 kcal/mol as the electrostatic effects attracting the negatively charged ligand and positive residues in the binding cleft decay. Contact between the ligand and specific residues on the periphery of the binding cleft lower this free energy barrier. R684 contacts the ligand's α-carboxylate (i = 73), lowering the free energy by ~2 kcal/mol, and the S652 side chain hydrogen bonds with the ligand (i = 61), lowering the free energy by ~1 kcal/mol. Notably, K449 contacts the ligand (i = 50) and passes it into the binding pocket. As the ligand enters from the ξ_1 side of the binding cleft, it interacts with three separate residues that stabilize a metastable transition state (Figure 2G) in which (1) the ligand's α-carboxylate coordinates the amine of Y450, (2) the ligand's amine interacts with the hydroxyl side chain of S652, and (3) the ligand's γ-carboxylate contacts K449 (i =32). This metastable interaction decreases the free energy barrier by ~3 kcal/mol. The α-carboxylate shifts into the binding pocket to contact R485 (i = 27), whereas the γ-carboxylate rotates downward to contact S654 and T655 (i = 13). Interactions that lock the LBD closed, including lobe 1- lobe 2 interactions between S652 and G451 (i = 24) and the salt bridge between K730 and D728 in the hinge region (i = 14), raise the free energy by ~2 kcal/mol.

Similarly in pathway 2 (Figure 5), attractive protein-ligand interactions plateau at ~10 Å (i = 102). The ligand first contacts the LBD at R453 on the ξ_1 side, lowering the free energy barrier by ~ 5 kcal/mol. R661 contacts the γ-carboxylate (i = 29), decreasing the free energy by ~6 kcal/mol. R485 rotates out of the binding pocket via rotations of +130°, +20°, −124°, and −61° around the R485 sidechain's χ_1, χ_2, χ_3, and χ_4 torsion angles, respectively (Figure 5 F, K) to coordinate the γ-carboxylate (i = 17). Glutamate moves into the binding pocket while its γ-carboxylate is coordinated by R485, and then flips downward so that the γ-carboxylate is coordinated by R485, and then flips downward so that γ-carboxylate is coordinated by R485, and then flips downward so that γ-carboxylate contacts S654, whereas the α-carboxylate flips up to contact R485 (i = 13). The LBD locks closed as the D651-S652 peptide bond flips (i = 13) and the K730-D728 salt bridge forms (i = 8). These interactions that close the LBD do not raise the free energy as in pathway 1; however, the final ligand-bound complex (i = 0) increases the free energy by ~3 kcal/mol.

The total binding free energy is given by: $\Delta G_{\mathrm{bind}}=\Delta G_0+\Delta G_N+\sum_{i=0}^{N-1}\Delta G_{i,i+1}$, where $\Delta G_{i,i+1}$ is the relative free energy difference between the system at state i and state i + 1. ΔG_0 is the free energy difference between the initial state and the unbiased ensemble of bound protein-ligand conformations. ΔG_N, likewise, is the free energy difference between the final state and the unbiased ensemble of apo protein and free ligand conformations. Assuming the initial (i = 0) and final (i = N) states of the binding pathway are well sampled, ΔG_0 and ΔG_N may be small. Alternatively, ΔG_0 and ΔG_N may be calculated by methods that

estimate the free energy of restraining the orientational, conformational, and translational change in both the protein and ligand during binding.[7]

The overall free energy difference between the initial and final state, $\sum_{i=0}^{N-1} \Delta G_{i,i+1}$, is −5.8 kcal/mol in pathway 1 and −8.8 kcal/mol in pathway 2, close to the experimentally measured binding free energy of −8.3 kcal/mol (IC_{50}) derived from competition assays of radiolabeled AMPA with glutamate.[26] Discrepancies in the calculated free energy values may be due to differences in the initial and final protein and ligand conformations between the two pathways, undersampling of state-to-state transitions, and inherent difficulties of free energy estimation in high dimensional spaces. The free energy difference between the end points may be compared to the experimental binding free energies if these discrepancies are small and the end points are representative of the ligand-bound and ligand-free ensembles. The free energies of the final ligand-bound complex are slightly higher than the free energy minima detected along the binding pathways. Previous simulations have also reported a mismatch between the free energy minimum and the ligand-bound crystal structure.[7,29] This mismatch may be due to a relaxation of the closed LBD to a slightly more open state when placed in a solvated simulation system.

Conclusions

In the present study, we have used a “chain of states” approach to probe glutamate binding in the AMPA receptor. The binding pathways converged after a few hundred nanoseconds of simulation time, whereas unbiased simulations typically require simulation times on the order of tens of microseconds to sample binding events in proteins which have similar on-rates ($k_{on} \sim 10^7\ M^{-1}\ s^{-1}$)[5]. Metastable interactions between the ligand and positively charged residues on helix F (R660, R661), R684, K660, and R453 lower the free energy barrier during ligand binding, and form local minima in the free energy landscape. The converged glutamate binding pathways indicate that the ligand binds either via the ξ_1 side of the LBD or the space formed between K449 and S652.

The string method approach has several limitations. Most notably, because the algorithm only moves images down an energy gradient, intermediate states can fall into local minima and become “trapped”, requiring several different initial interpolations to sample multiple transition pathways. It is difficult to sample all possible transition pathways using the string method, and other low energy pathways for glutamate binding may exist, distinct from the two observed pathways.

Free energy profiles calculated along the binding pathways demonstrate that specific residue-ligand interactions outside of the binding pocket contribute substantially to the energetics of ligand binding. Why might a protein domain contain such low affinity binding sites that do not engage the ligand in its stably bound form? We speculate that these interactions may serve to position the ligand into conformations that are more competent to bind. If this is true, metastable binding sites can facilitate the diffusion of ligands across narrow, tight spaces, like the recessed binding pocket of the AMPA receptor LBD. In general, proteins have adopted a wide range of strategies to transfer molecules to locations

where they can be acted upon, so it is not implausible that low affinity binding sites situated in strategically positioned locations may be another general feature for molecular transport.

Supplementary Material

Refer to Web version on PubMed Central for supplementary material.

Acknowledgments

This study used resources provided by the Maryland Advanced Research Computing Center (MARCC) at Johns Hopkins University. This work was supported by the National Institutes of Health grant R01GM094495 (to A.Y.L.).

References

1. Traynelis SF, Wollmuth LP, McBain CJ, Menniti FS, Vance KM, Ogden KK, Hansen KB, Yuan H, Myers SJ, Dingledine R. Glutamate Receptor Ion Channels: Structure, Regulation, and Function. Pharmacol Rev. 2010; 62:405–496. [PubMed: 20716669]
2. Mayer ML. Glutamate Receptors at Atomic Resolution. Nature. 2006; 440:456–462. [PubMed: 16554805]
3. Mayer ML. Structure and Mechanism of Glutamate Receptor Ion Channel Assembly, Activation and Modulation. Curr Opin Neurobiol. 2011; 21:283–290. [PubMed: 21349697]
4. Shan Y, Kim ET, Eastwood MP, Dror RO, Seeliger MA, Shaw DE. How Does a Drug Molecule Find Its Target Binding Site? J Am Chem Soc. 2011; 133:9181–9183. [PubMed: 21545110]
5. Dror RO, Pan AC, Arlow DH, Borhani DW, Maragakis P, Shan Y, Xu H, Shaw DE. Pathway and Mechanism of Drug Binding to G-Protein-Coupled Receptors. Proc Natl Acad Sci U S A. 2011; 108:13118–13123. [PubMed: 21778406]
6. Shaw, DE., Dror, RO., Salmon, JK., Grossman, JP., Mackenzie, KM., Bank, JA., Young, C., Deneroff, MM., Batson, B., Bowers, KJ., et al. Proceedings of the Conference on High Performance Computing Networking, Storage and Analysis. Vol. SC '09. ACM; New York, NY, USA: 2009. Millisecond-Scale Molecular Dynamics Simulations on Anton; p. 39:1-39:11.
7. Lau AY, Roux B. The Hidden Energetics of Ligand-Binding and Activation in a Glutamate Receptor. Nat Struct Mol Biol. 2011; 18:283–287. [PubMed: 21317895]
8. Maragliano L, Fischer A, Vanden-Eijnden E, Ciccotti G. String Method in Collective Variables: Minimum Free Energy Paths and Isocommittor Surfaces. J Chem Phys. 2006; 125:24106. [PubMed: 16848576]
9. Pan AC, Sezer D, Roux B. Finding Transition Pathways Using the String Method with Swarms of Trajectories. J Phys Chem B. 2008; 112:3432–3440. [PubMed: 18290641]
10. Fiser A, Sali A. ModLoop: Automated Modeling of Loops in Protein Structures. Bioinformatics. 2003; 19:2500–2501. [PubMed: 14668246]
11. Krivov GG, Shapovalov MV, Dunbrack RL. Improved Prediction of Protein Side-Chain Conformations with SCWRL4. Proteins. 2009; 77:778–795. [PubMed: 19603484]
12. Mackerell AD, Feig M, Brooks CL. Extending the Treatment of Backbone Energetics in Protein Force Fields: Limitations of Gas-Phase Quantum Mechanics in Reproducing Protein Conformational Distributions in Molecular Dynamics Simulations. J Comput Chem. 2004; 25:1400–1415. [PubMed: 15185334]
13. MacKerell AD, Bashford D, Bellott M, Dunbrack RL, Evanseck JD, Field MJ, Fischer S, Gao J, Guo H, Ha S, et al. All-Atom Empirical Potential for Molecular Modeling and Dynamics Studies of Proteins. J Phys Chem B. 1998; 102:3586–3616. [PubMed: 24889800]
14. Jorgensen WL, Chandrasekhar J, Madura JD, Impey RW, Klein ML. Comparison of Simple Potential Functions for Simulating Liquid Water. J Chem Phys. 1983; 79:926–935.
15. Brooks BR, Brooks CL, MacKerell AD, Nilsson L, Petrella RJ, Roux B, Won Y, Archontis G, Bartels C, Boresch S, et al. CHARMM: The Biomolecular Simulation Program. J Comput Chem. 2009; 30:1545–1614. [PubMed: 19444816]

16. Meng Y, Shukla D, Pande VS, Roux B. Transition Path Theory Analysis of c-Src Kinase Activation. Proc Natl Acad Sci U S A. 2016; 113:9193–9198. [PubMed: 27482115]
17. Zhu F, Hummer G. Pore Opening and Closing of a Pentameric Ligand-Gated Ion Channel. Proc Natl Acad Sci U S A. 2010; 107:19814–19819. [PubMed: 21041674]
18. Lev B, Murail S, Poitevin F, Cromer BA, Baaden M, Delarue M, Allen TW. String Method Solution of the Gating Pathways for a Pentameric Ligand-Gated Ion Channel. Proc Natl Acad Sci U S A. 2017; 114:E4158–E4167. [PubMed: 28487483]
19. Ovchinnikov V, Cecchini M, Vanden-Eijnden E, Karplus MA. Conformational Transition in the Myosin VI Converter Contributes to the Variable Step Size. Biophys J. 2011; 101:2436–2444. [PubMed: 22098742]
20. Chodera JD, Mobley DL, Shirts MR, Dixon RW, Branson K, Pande VS. Alchemical Free Energy Methods for Drug Discovery: Progress and Challenges. Curr Opin Struct Biol. 2011; 21:150–160. [PubMed: 21349700]
21. Dickson A, Warmflash A, Dinner AR. Nonequilibrium Umbrella Sampling in Spaces of Many Order Parameters. J Chem Phys. 2009; 130:74104.
22. Vanden-Eijnden E, Venturoli M. Markovian Milestoning with Voronoi Tessellations. J Chem Phys. 2009; 130:194101. [PubMed: 19466815]
23. Maragliano L, Vanden-Eijnden E, Roux B. Free Energy and Kinetics of Conformational Transitions from Voronoi Tessellated Milestoning with Restraining Potentials. J Chem Theory Comput. 2009; 5:2589–2594. [PubMed: 20354583]
24. Kumar S, Rosenberg JM, Bouzida D, Swendsen RH, Kollman PA. THE Weighted Histogram Analysis Method for Free-Energy Calculations on Biomolecules. I. The Method. J Comput Chem. 1992; 13:1011–1021.
25. Souaille M, Roux B. Extension to the Weighted Histogram Analysis Method: Combining Umbrella Sampling with Free Energy Calculations. Comput Phys Commun. 2001; 135:40–57.
26. Armstrong N, Gouaux E. Mechanisms for Activation and Antagonism of an AMPA-Sensitive Glutamate Receptor: Crystal Structures of the GluR2 Ligand Binding Core. Neuron. 2000; 28:165–181. [PubMed: 11086992]
27. Hogner A, Greenwood JR, Liljefors T, Lunn ML, Egebjerg J, Larsen IK, Gouaux E, Kastrup JS. Competitive Antagonism of AMPA Receptors by Ligands of Different Classes: Crystal Structure of ATPO Bound to the GluR2 Ligand-Binding Core, in Comparison with DNQX. J Med Chem. 2003; 46:214–221. [PubMed: 12519060]
28. Menuz K, Stroud RM, Nicoll RA, Hays FA. TARP Auxiliary Subunits Switch AMPA Receptor Antagonists into Partial Agonists. Science. 2007; 318:815–817. [PubMed: 17975069]
29. Dai J, Zhou HX. Semiclosed Conformations of the Ligand-Binding Domains of NMDA Receptors during Stationary Gating. Biophys J. 2016; 111:1418–1428. [PubMed: 27705765]
30. Lau AY, Roux B. The Free Energy Landscapes Governing Conformational Changes in a Glutamate Receptor Ligand-Binding Domain. Structure. 2007; 15:1203–1214. [PubMed: 17937910]

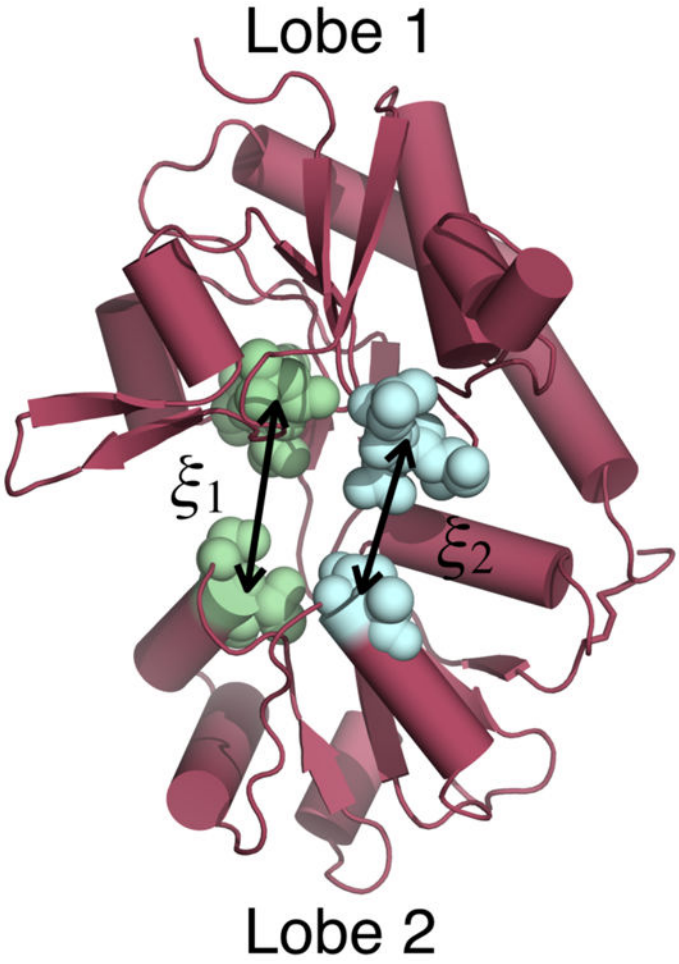

Figure 1.

Opening and closing of the GluA2 LBD is described by the two-dimensional order parameter (ξ_1, ξ_2). ξ_1 is the center of mass distance between residues 479–481 on lobe 1 and residues 654–655 on lobe 2 (green). ξ_2 is the center of mass distance between residues 401–403 on lobe 1 and residues 686–687 on lobe 2 (cyan). Together, they indicate the degree of cleft closure in the open-to-closed transition of the LBD as in Lau et al.[7,30]

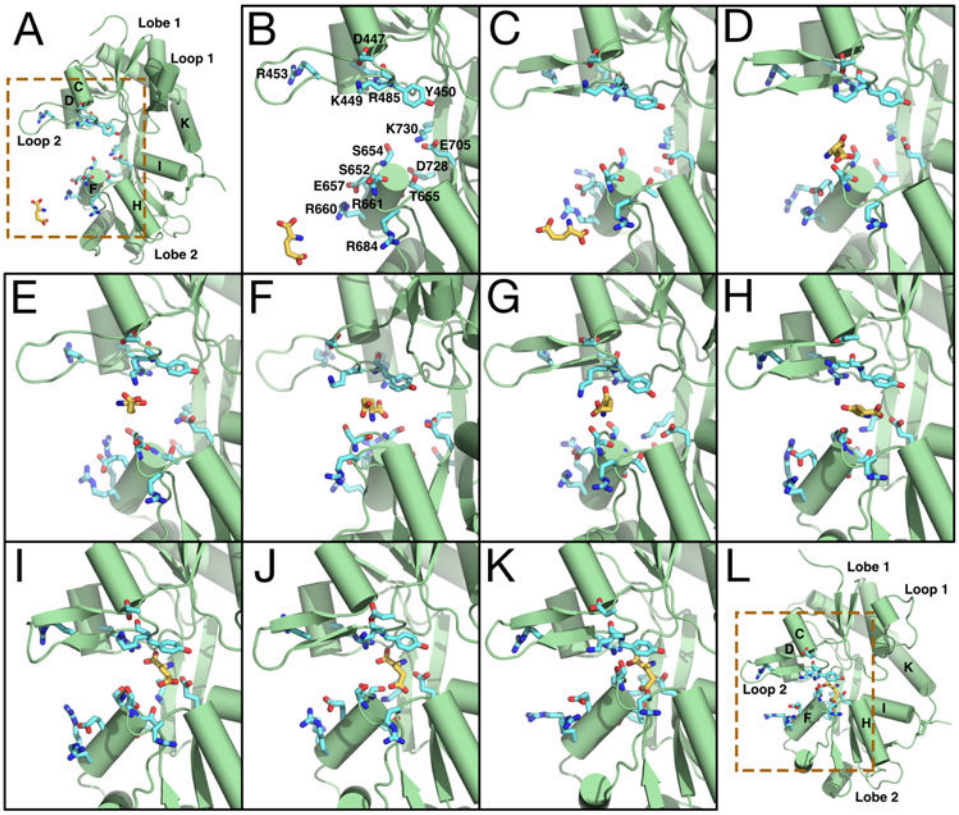

Figure 2.

Locally optimized binding intermediates in pathway 1. (**A**) The initial conformation used in the string method for pathway 1 contains an open LBD (ξ_1, ξ_2) = (14.1 Å, 13.9 Å) and a ligand separated by bulk solvent. (**B**) Close-up view of (**A**). (**C**) Glutamate contacts R684 on lobe 2. (**D**) The S652 hydroxyl sidechain hydrogen bonds with the amine of glutamate. (**E**) K449 interacts with the ligand's γ-carboxylate (**F**) Glutamate shifts into the binding pocket. (**G**) Glutamate forms three contacts across lobe 1 and lobe 2 of the LBD. (1) The α-carboxylate contacts the backbone amine of Y450. (2) The amine interacts with the S652 hydroxyl side chain. (3) K449 contacts the γ-carboxylate. (**H**) Glutamate is coordinated by the aromatic sidechain of Y450, aligning with the α-carboxylate proximal to R485. (**I**) The α-carboxylate contacts R485 on lobe 1 and E705 on lobe 2. (**J**-**K**) The LBD closes further around the ligand (ξ_1, ξ_2) = (9.5 Å, 8.3 Å) as the γ-carboxylate contacts the backbone amines of S654 and T655. (**L**) Expanded view of (**K**).

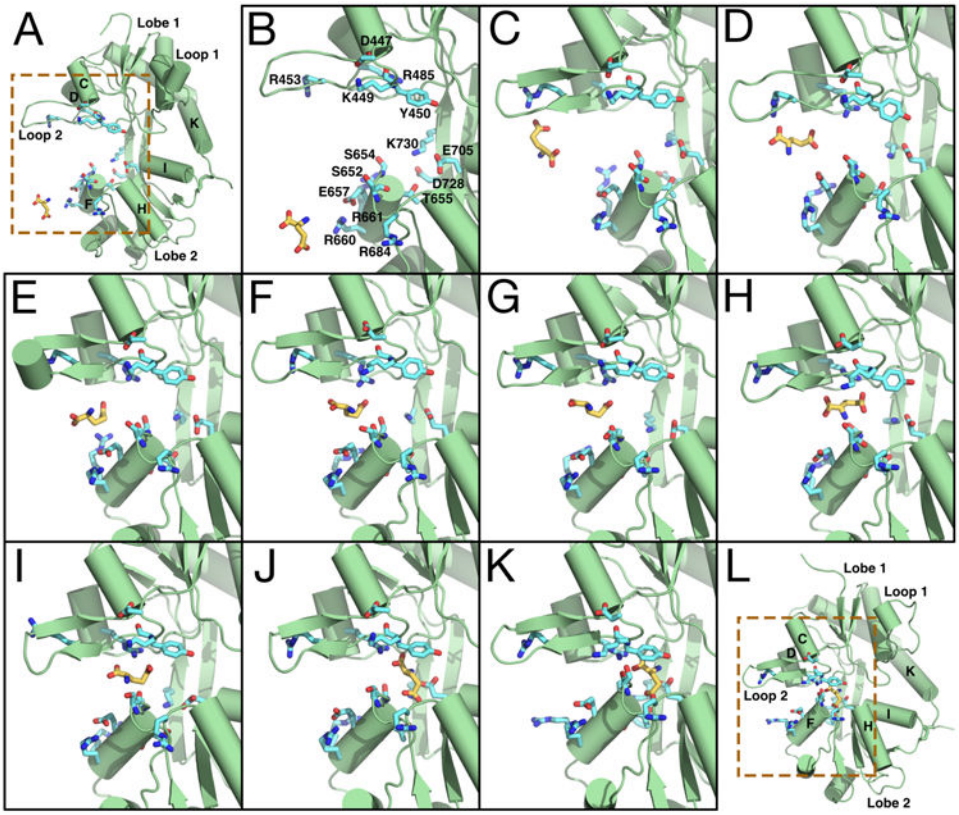

Figure 3.

Locally optimized binding intermediates in pathway 2. (**A**) The initial conformation used in the string method for pathway 2 contains an open LBD (ξ_1, ξ_2) = (14.1 Å, 13.9 Å) and a ligand separated by bulk solvent. (**B**) Close-up view of (**A**). (**C-D**) Glutamate contacts R453 on the ξ_1 side of lobe 1. (**E**) R661 contacts the ligand's γ-carboxylate (**F**) R485 flickers out of the binding pocket to contact the γ-carboxylate. (**G-I**) R485 relaxes toward the binding pocket while coordinating the ligand's γ-carboxylate. (**J**) The γ-carboxylate flips downward into the binding pocket, while the α-carboxylate flips upward to contact R485. The amine contacts E705 on lobe 2. (**K**) The LBD closes further around the ligand (ξ_1, ξ_2) = (9.5 Å, 8.3 Å) as the γ-carboxylate coordinates the backbone amines of S654 and T655. (**L**) Expanded view of (**K**).

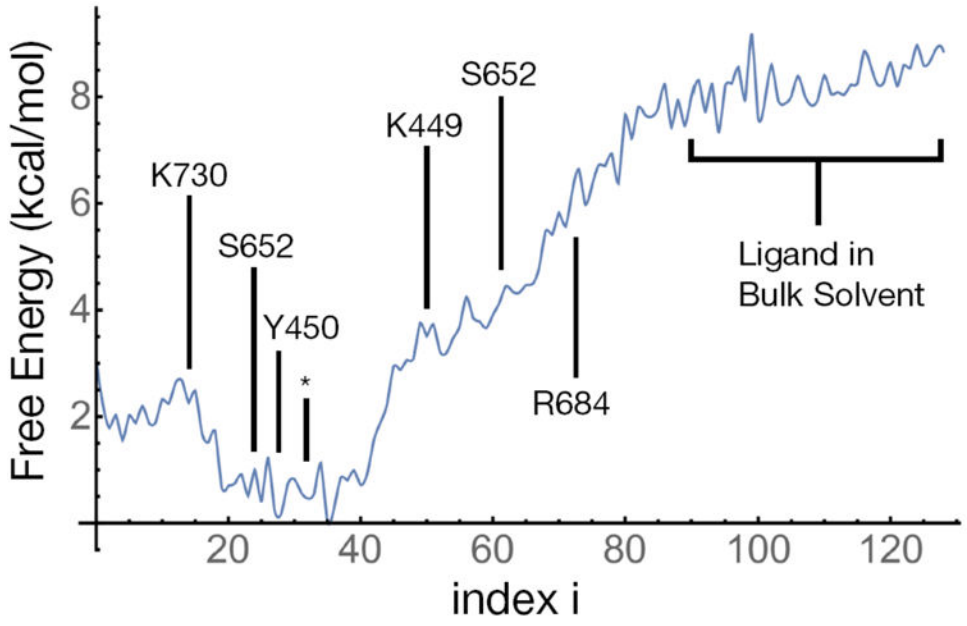

Figure 4.

The free energy profile along binding pathway 1. The indices refer to images, or conformations, along pathway 1, calculated by the string method. The free energy was calculated by Voronoi tessellating the phase space of the collective variables and performing umbrella sampling. At images (i = 90 – 129) the ligand is in bulk solvent, and at image 0, the ligand is fully bound within the LBD, in the crystallographic conformation. Protein-ligand interactions that change the energetics of ligand binding are labeled. The asterisk (*) indicates an image that contains a metastable intermediate consisting of the following interactions: ligand α-carboxylate to Y450 backbone amine, ligand amine to S652 hydroxyl side chain, and ligand γ-carboxylate to K449 sidechain.

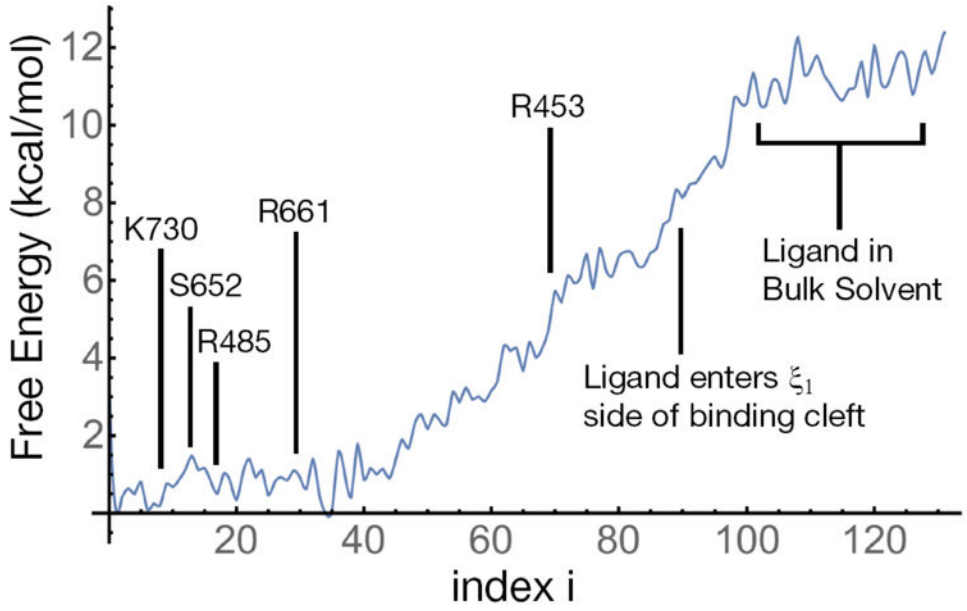

Figure 5.

The free energy profile along binding pathway 2. The indices refer to images, or conformations, along pathway 2, calculated by the string method. The free energy was calculated by Voronoi tessellating the phase space of the collective variables and performing umbrella sampling. At images (i = 102–131) the ligand is in bulk solvent, and at image 0, the ligand is fully bound within the LBD, in the crystallographic conformation. Protein-ligand interactions that change the energetics of ligand binding are labeled.